Applied Catalysis B: Environmental 84 (2008) 87–93

Contents lists available at ScienceDirect

Applied Catalysis B: Environmental

journal homepage: www.elsevier.com/locate/apcatb

Ag promotion of TiO_2-anatase disinfection capability: Study of *Escherichia coli* inactivation

A. Kubacka *, M. Ferrer, A. Martínez-Arias, M. Fernández-García

Instituto de Catálisis y Petroleoquímica (CSIC), C/Marie Curie 2, 28049-Madrid, Spain

ARTICLE INFO

Article history:
Received 5 January 2008
Received in revised form 18 February 2008
Accepted 21 February 2008
Available online 26 February 2008

Keywords:
Photocatalysis
TiO_2
Anatase
Silver
Disinfection
E. coli

ABSTRACT

In this report we investigate the promotion of the TiO_2-anatase disinfection capability by addition of silver. Ag–TiO_2 systems were prepared by two different methods, impregnation and photodeposition, and their anti-microbial properties analyzed as a function of the silver content using *Escherichia coli* as a benchmark microorganism. Both Ag–TiO_2 series of samples display maximum photokilling activity for a 1 wt.% silver loading but behave very differently for higher silver loadings. The noble metal roles played on the *E. coli* inactivation and their physical grounds were analyzed by a multitechnique approach using XRD, and Raman, UV–vis and electron paramagnetic resonance (EPR) spectroscopies.

1. Introduction

Nowadays, there is a great concern to guarantee the future sources and settle securely the provision of clean drinking water. Current challenges not only deal with chemical-related pollution risks in industrialized countries but also with the worldwide spread of biological risks connected with traditional sources as well as bioterrorism. Conventional treatment/disinfection technologies such as ozonation or chlorination have some limitations as, for example, ozone does not remain in water very long and the use of chlorine as a water disinfectant may lead to its potential reaction with organic matter and formation of toxic by-products (as, for example, the carcinogen trihalomethanes) [1]. Novel technologies, like advanced oxidation processes, can open a window to solve these problems. Among them, photocatalysis emerges as a fruitful promise due to its potential to attack chemical/biological risks without matter of their chemical nature/composition. Universal applicability together with the absence of by-products and necessity to be released to the media along with, finally, the impossibility of developing resistance by part of the microorganism are key, positive aspects inherent to this technology. TiO_2-anatase is by far the most widely used photocatalyst; it is a wide bandgap (3.2 eV) semiconductor which under UV illumination generates energy-rich electron–hole pairs able to degrade chemicals and/or cell components of microorganisms, and rendering innocuous products, mainly water and carbon dioxide [2–4].

TiO_2 photoactivity is strongly influenced by the presence of noble metals [5]. Silver has received attention in the context of disinfection since 1985, when Matsunga et al. first reported its use [6]. Further work on the field provides evidence of several physico-chemical phenomena of importance to interpret photokilling activity. On first place, silver has a well-known bactericidal capability by its own. Ag(I) ions are strong electron donors primarily involved in interactions with cell proteins through sulphydryl groups. Silver nanoclusters release Ag(0) and both chemical species Ag(I) ions and Ag(0) atoms have shown to rapidly kill bacteria and fungi [7–10]. Silver can also play roles associated to its presence at the titania surface. This metal strongly influences charge separation upon light absorption [5,11] affecting in this way photo-chemical activity [12,13]. Besides that, silver can change the surface characteristics of titania at local level; for similar metals, like Cu, loadings ca. 5 wt.%, can drive to measurable variations in the point of zero charge (PZC), altering in this way the initial steps of the microorganism interaction (adhesion) to the catalyst surface [14].

In this paper, we seek for a better understating of the silver interaction with nanosize anatase and the potential effects in

* Corresponding author. Fax: +34 91 585 4760.
E-mail address: a.kubacka@icp.csic.es (A. Kubacka).

0926-3373/$ – see front matter © 2008 Elsevier B.V. All rights reserved.
doi:10.1016/j.apcatb.2008.02.020

the anti-microbial properties of the system. Silver was deposited using two methods, impregnation and photodeposition, and the performance of the systems in the photokilling of *E. coli* as a function of the silver loading of the material has been studied. *E. coli* is a well-known pathogen commonly involved in food contamination and is also widely used in reference tests to measure bactericidal properties [4]. Kiwi et al. [15,16] showed that *E. coli* membrane components like lipo-polysaccharides and phospholipids favorably compete for the scavenging of holes with the electron–hole recombination occurring in titania particles. The initial membrane cell damage is subsequently followed by oxidative attack to internal cell components, ultimately resulting in cell death. These authors also provide evidence for a direct link between the hole scavenging probability and the *E. coli* inactivation. Other valuable works analyzed the influence of light-related physical phenomena [17–19] and showed that hole-related OH-type radicals are directly involved in the inactivation process [20]. To test all these silver-mediated effects, the photo-chemical properties of our Ag–TiO_2 systems have been analyzed using a multitechnique approach which may allow (*vide infra*) a rationalization of their disinfection potential.

2. Experimental procedure

2.1. Samples synthesis and characterization

As described elsewhere, TiO_2 was prepared by combined sol–gel/microemulsion giving an oxide solid with anatase structure after calcination at 723 K during 2 h [21,22]. Silver with a final content of the solid of 0.5–2.5 wt.% (metal basis) was deposited by: (i) the incipient wetness impregnation of the calcined titania using 0.6 ml g^{-1} of a $AgNO_3$ (Merck) aqueous solution. After drying at 383 K, the impregnated samples were calcined at 723 K under air. The second method was (ii) photodeposition; an aqueous suspension of titania (5 g l^{-1}) in presence of 10 v/v% of ethanol as a sacrificial agent was irradiated (Hg lamp, 400 W) for 4 h under a nitrogen flow. Photodesposited samples were subsequently subjected to filtration and overnight drying at 383 K. Sample labels, main preparation and physico-chemical properties of Ag-containing samples are included in Table 1. Sample labels indicate the Ag content of the materials as measured by Atomic Absorption with an error of 15%; the suffix F denotes samples prepared by photodeposition.

The BET surface areas and average pore sizes were measured by nitrogen physisorption (Micromeritics ASAP 2010). Particle sizes were measured with XRD using the Scherrer equation. XRD profiles were obtained with a Seifert diffractometer using Ni-filtered Cu Kα radiation. UV–vis diffuse reflectance spectroscopy experiments were performed with a Shimadzu UV2100 apparatus and Raman data were acquired using a Bruker RFS-100 FT-Raman spectrometer. Ag lixiviation after reaction was analyzed by using inductive coupled plasma-ICP (PerkinElmer, Optima 3300 DV).

Table 1
Main characterization results of Ag–TiO_2 samples

Sample	S_{BET} (m^2 g^{-1})	Crystal size (nm)[a]	Direct/indirect band gap (eV)[b]
TiO_2	73.6	9.7	3.1/3.5
0.5Ag	82.0	9.6	3.0/3.5
1.0Ag	83.8	9.6	3.1/3.4
2.5Ag	71.2	9.9	3.0/3.4
1.0AgF	80.1	9.9	3.1/3.5
2.5AgF	77.4	9.8	3.2/3.6

[a] For anatase-type structure. Measured by XRD using Scherrer equation.
[b] Details of the analysis performed for this determination can be found in Ref. [32].

2.2. Photo-chemical viability assays

The microorganism used in this study was *E. coli* CECT 101, which was maintained according to the recommendations of the manual of the Spanish Type Culture Collection (CECT; http://www.uv.es/cect/). Cells were streaked from a glycerol stock onto a Luria-Bertani (LB) agar plate, grown overnight at 37 °C and subsequently used for photo-chemical cell viability assays. To study the anti-microbial activity of the TiO_2-based catalysts, two suspensions were prepared. The first suspension was an aqueous solution of the material at 1 mg ml^{-1} using sterilized water. The second contained 10 μl of microbial cells (ca. 10^9 CFU ml^{-1}) suspended in 1 ml broth solution. Grow cultures were prepared as described elsewhere [23]. Aliquots of both suspensions were added to a 4 ml quartz cubic cell (5 mm of optical path length) containing 1 ml of sterilized water. The oxide-cell slurry (0.1–2.0 g-TiO_2 l^{-1}) was placed in the UV spectrometer chamber (UVIKON 930) and irradiated with a UV-B light of 280 nm for different periods of time under continuous agitation. A 0.5 W m^{-2} power was measured as the sample place; this accounts for a maximum radiation energy fluence (power × time) below 1 kJ m^{-2} during the experiment. Such radiation dose has not significant influence on cell viability [24]. After irradiation and for different time intervals, aliquots of 100 μl were transferred to a 10 ml LB broth test tube. The order of cell dilution at this stage was 10^{-2}. Loss of viability after each exposure time was determined by the viable count procedure on LB agar plates after serial dilution (10^{-2} to 10^{-5}). All plates were incubated at 37 °C for 24 h prior to enumeration. A minimum of three experiments was carried out to determine anti-microbial activity. The inactivation curves showed two decay processes corresponding to the initial and final part of the experiments which were modeled by using two exponential decay equations, according to the model described elsewhere [25]. The corresponding inactivation rates were used to compare the catalysts performance.

2.3. EPR experiments

The EPR measurements were done with a Bruker ER200D spectrometer operating in the X-band and calibrated with a DPPH standard. For the 5,5-dimethyl-1-pyrroline *N*-oxide (DMPO) spin trapping EPR experiments, the samples were suspended in water (at a concentration of 1 g l^{-1}) and were sonicated for 4 min. An aqueous solution (0.01 M) of DMPO spin trap (supplied by Sigma) was prepared and kept on ice during the whole set of experiments. Bidistilled water (Elix-10) was employed for these preparations. 100 μl of the solid suspension and 100 μl of the DMPO solution were mixed into an EPR flat quartz cell under atmospheric air and irradiated at different times, through a filter with a cut-off at ca. 220 nm, with UV-type lamps identical to those employed for the photoactivity tests, being then immediately transferred to the spectrometer cavity for EPR analysis. A small radical concentration decay (of ca. 5% on average) was observed in the dark during the course of spectrum recording. The latter were obtained at 298 K at ca. 9.75 GHz microwave frequency, 19.5 mW microwave power, 100 kHz modulation frequency, 2 G modulation amplitude and 2×10^5 spectrometer gain. No significant signal saturation was observed in those conditions. Blank experiments were also performed over mixtures of 100 μl of the DMPO solution and 100 μl of water to check the absence of radical formation in the absence of solid under the employed conditions.

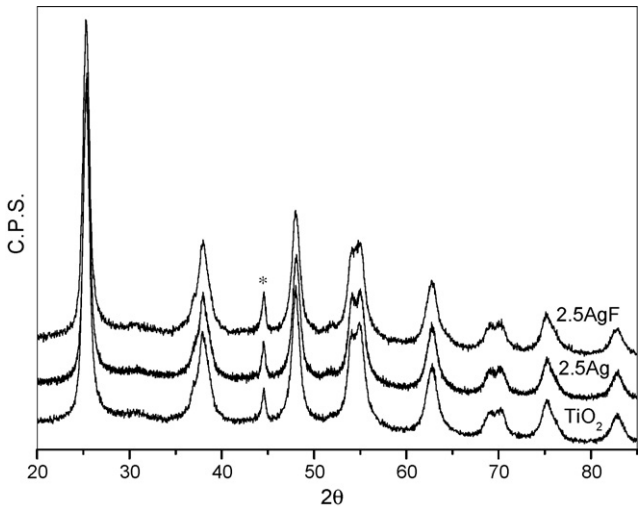

Fig. 1. XRD patterns for selected Ag–TiO_2 samples. The asterisk mark indicates a sample-holder contribution.

Another set of experiments was performed at 77 K using a conventional spectroscopic quartz tube cell (4 mm o.d.) employed for studies of solid samples. Aliquots of the sample (ca. 30 mg) were thoroughly treated under high vacuum conditions at room temperature and then irradiated with UV-lamps (maximum at 280 nm) during 15 min at 77 K. Experiments followed with chemisorption of oxygen (upon introduction in the cell of a 50 μmol g^{-1} dose) at 77 K followed by UV-type irradiation in the presence of oxygen at 77 K and final thorough outgassing at 77 K.

3. Results

In Table 1 we summarize the main characteristics of the TiO_2-based materials synthesized; as can be observed in this table, the presence of silver, irrespective of the preparation method, does not change appreciably the surface area and primary particle size of the oxide component. X-ray diffraction (Fig. 1) and Raman spectroscopy (results not shown) give evidence that all samples contain titania in the anatase structure (JCPDS-84-1286) with additional presence of brookite traces, as has been previously reported for the single oxide TiO_2 reference [22,26]. These results allow to say that, to a first approximation, the preparation of the Ag–TiO_2 systems does not alter the structural (anatase:brookite ratio) and morphological (primary particle size, surface area) characteristics of the oxide component.

Fig. 2 shows the UV–vis spectra of the samples, which display a practically invariant absorption threshold onset of the TiO_2-anatase component (Table 1) together with some visible-range silver-related contribution(s). In Fig. 2A we can see that impregnated samples only show a minor contribution close to the anatase absorption edge while photodeposited samples display a broad feature centred at ca. 515 nm, ascribable to the Ag(0) surface plasmon [12]. As expected, silver chemical state appears to vary in our systems; in impregnated samples, the subsequent calcinations stabilizes the oxidized Ag(I) state while photoreduction leads, as expected, to the metallic state. In addition, Fig. 2B provides evidence of sample evolution under reaction for the photodeposited samples. Clearly, the silver component becomes oxidized. This is not uncommon; photo-chemical oxidation of noble metals deposited on titania has been shown to occur at the metal-support interface under the effect of the UV-light and reactant atmosphere [27] and has been proved here in a separate test. Accordingly, possibly both the light and charge exchange with the bacteria can alter the oxidation state of silver. The extent of this phenomenon depends on morphological properties (primary and secondary particle size; aggregation in the aqueous media) of the oxide [28] but seems nearly complete here for 1 wt.% samples (Fig. 2B). The ending result is that all samples will display an oxidized surface silver state under reaction, although the 2.5AgF sample could apparently maintain a metallic-like kernel.

The *E. coli* survival curves as a function of time for the different samples are presented in Fig. 3. Tests run here used a 280 nm

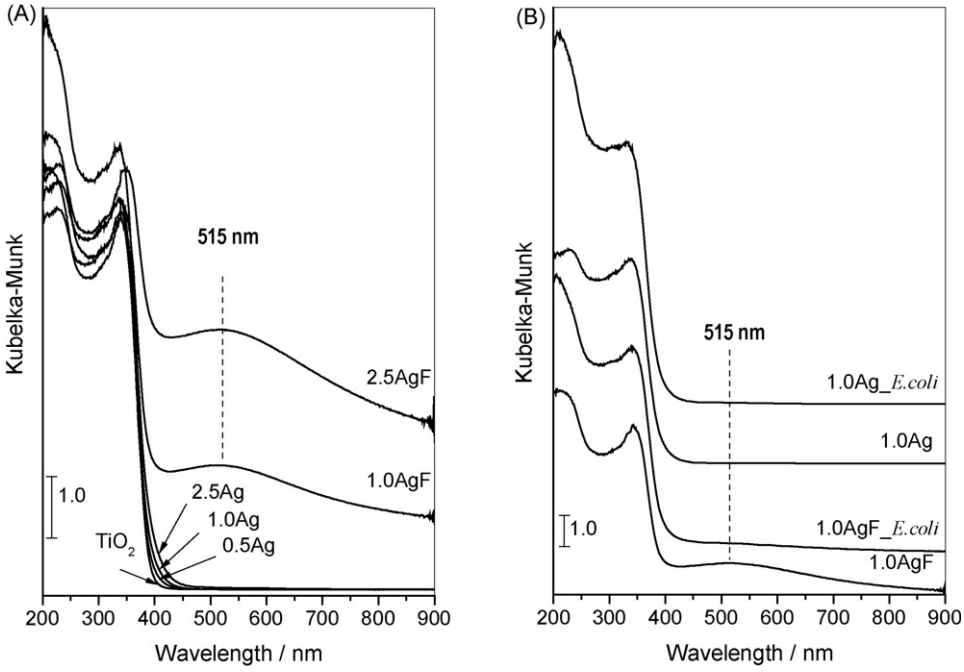

Fig. 2. UV–vis spectra of fresh (A) and comparison of some of these with used samples (referred to by employing ***_Ecoli*** suffixes) (B) samples. Used samples are scaled up and shown in comparison with fresh materials.

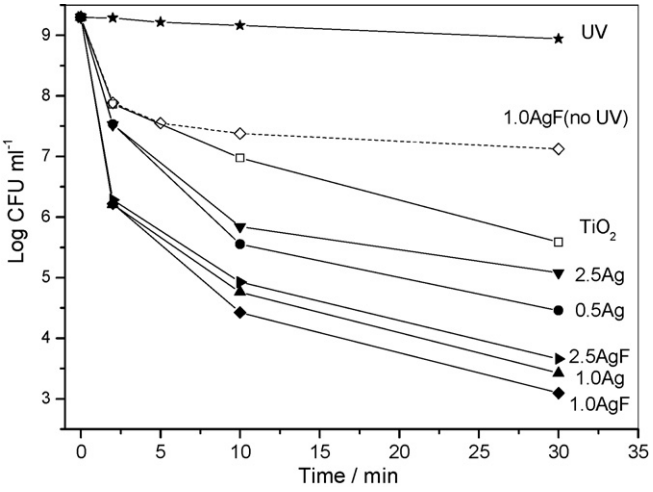

Fig. 3. Survival curves for ***E. coli*** as a function of the irradiation time for Ag–TiO_2 and reference samples.

source; previous results showed that using UV-B (as well as UV-A) light the photocatalyst plays an active role in the inactivation process [18]. Results on bare titania showed that anti-microbial activity is maximized with an oxide photocatalyst concentration in the 0.5–1.0 g-TiO_2 l^{-1} range, in accordance with previous reports [17,18,29]. Fig. 3 reports results using a 1.0 g l^{-1} and includes two reference tests; the first describes the UV-light effect on bacteria population while the second analyzed *E. coli* inactivation in presence of the 1.0AgF catalyst but absence of light. A similar dark-test was done with TiO_2 alone. All reference tests indicate the minimal effect of UV-light (due to the limited fluences used here) and silver by themselves, as will be discussed below. Presence of TiO_2-anatase is required to attain significant inactivation of the microorganism. All curves show, similarly to previous reports, a fast initial decay followed by a slow, tailing process characteristic of longer reaction times [18,30]. This latter decreasing inactivation rate is probably related to self-defense mechanisms of bacteria involving enzymes, catalase, and superoxide dismutase to limit oxidative stress [31], as well as the influence of lysed cell part as UV-light blocking agents and/or consumers of TiO_2-related radicals [25,30,31]. The plots in Fig. 3 provide evidence of the somewhat better performance of the photodeposited systems with respect to impregnated ones. This trend is more acute as the silver content of the material grows. An optimum concentration of 1 wt.% of silver appears common to both preparation procedures and leads to a ca. 6 logCFU units decrease by the end of the experiment. Table 2 summarizes the photokilling performance of the systems reporting the inactivation rate for the fast (K_f) and slow (K_s) steps of the curves showed in Fig. 3 and the maximum logCFU decrease (after 30 min). It can be noted that ICP analyses of post-reaction solutions using the 1 wt.% samples showed no significant silver lixiviation (detection limit for silver within our experimental conditions; 0.5 mg l^{-1}) after completion of the experiment.

Table 2
Fast (K_f) and slow (K_s) inactivation rates and maximum logCFU reduction observed for *E. coli* photokilling tests

Sample	K_f (min^{-1})	K_s (min^{-1})	Maximum logCFU
UV	0.01		0.3
1.0AgF (no light)	0.71	0.01	2.2
TiO_2	0.71	0.07	3.7
0.5Ag	0.88	0.05	4.8
1.0Ag	1.54	0.07	5.9
2.5Ag	0.88	0.04	4.2
1.0AgF	1.64	0.07	6.2
2.5AgF	1.64	0.03	5.7

Standard error in K values is ±20%. Standard error in logCFU values ±0.2 units.

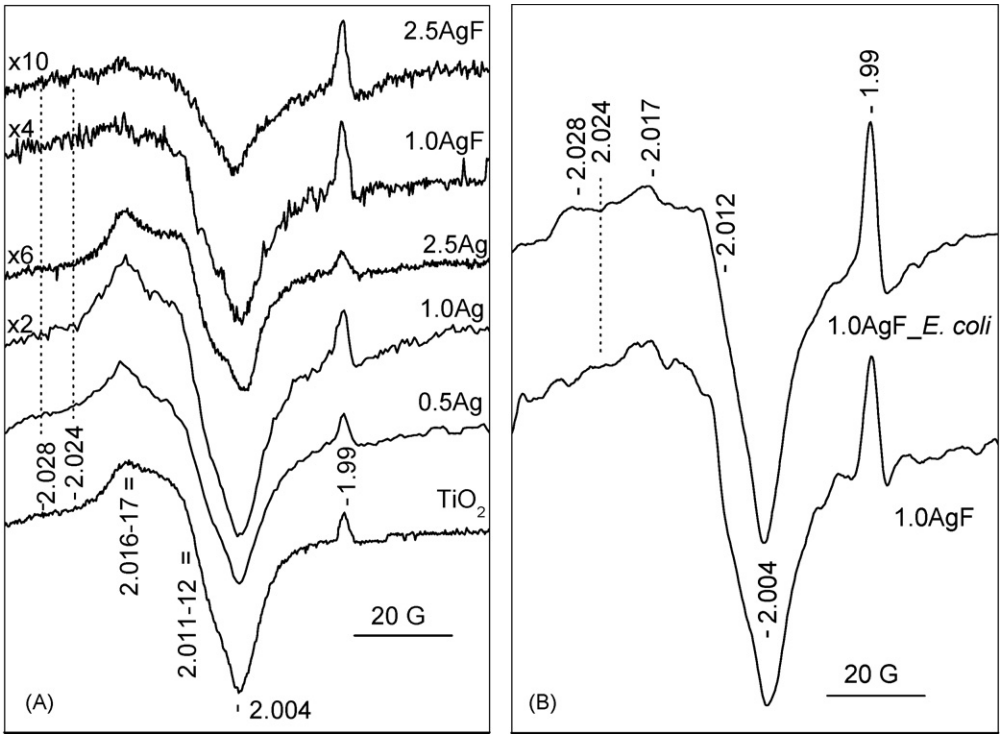

Fig. 4. EPR spectra at 77 K of the radicals formed upon UV irradiation of fresh (A) and comparison between fresh and used (denoted with a ***_Ecoli*** suffix) (B) samples in presence of oxygen.

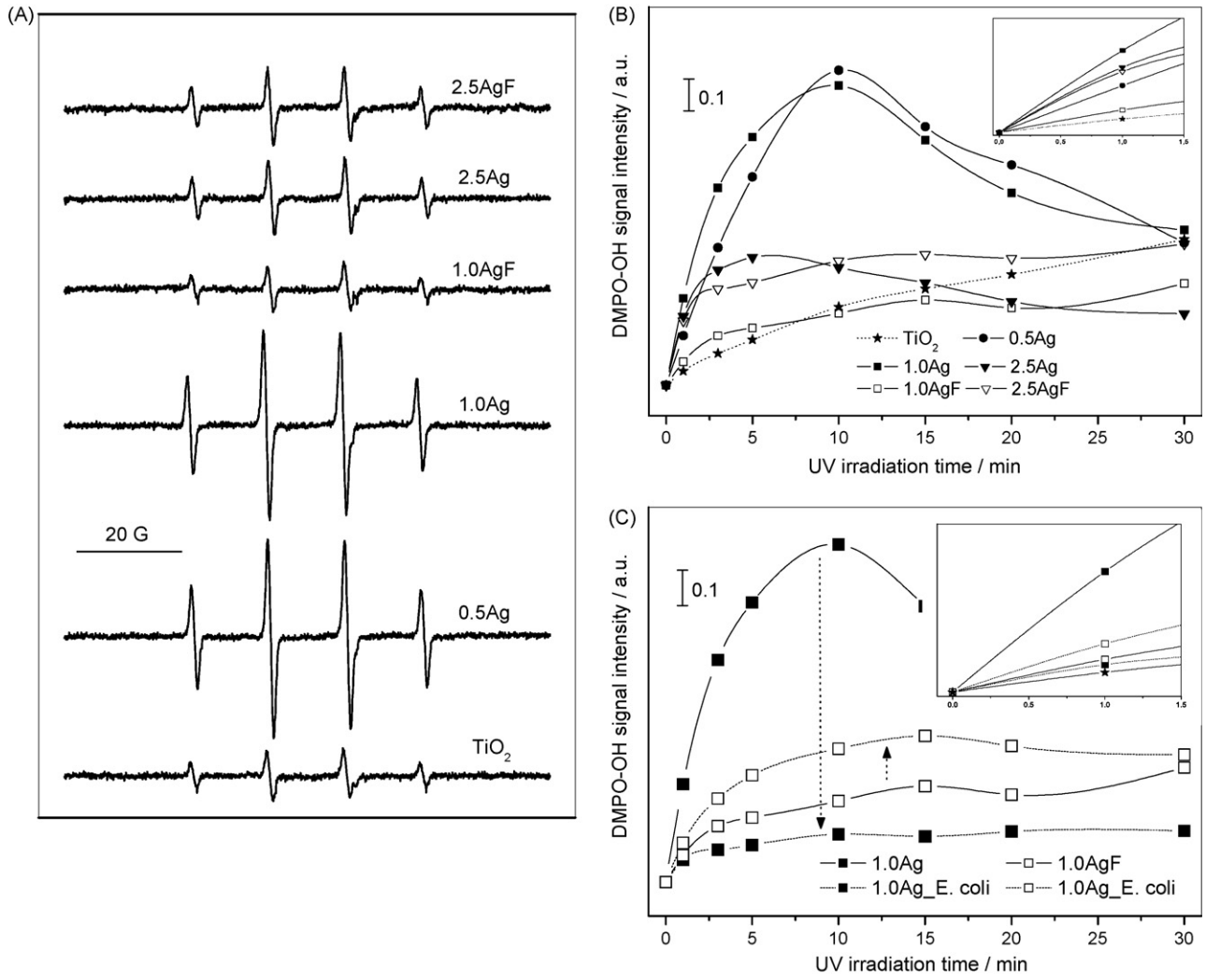

Fig. 5. (A) EPR spectra of DMPO-sample aqueous suspension after 10 min UV-light irradiation. (B) Evolution of the DMPO-OH signal intensity for Ag–TiO_2 and reference samples as a function of irradiation time. (C) As former plot but including fresh and used (referred to with ***Ecoli*** suffixes) samples. Inset in B and C shows an expanded view of the initial part.

To interpret the photokilling results presented above an EPR study of the electron and hole trapping capabilities of our samples has been undergone. While Fig. 4 presents a summary of the EPR results on samples outgassed and subsequently contacted with oxygen and UV-irradiated at 77 K, Fig. 5 displays results concerning DMPO-trapping studies performed at 298 K. It may be noted that presence of metallic silver may to some extent disturb EPR results by electrically absorbing microwave intensity (and thus decreasing to some extent the total EPR intensity). The analysis of the surface electron capture in presence of oxygen could provide a reasonable idea of the sample electron/hole trapping capability at the surface (e.g., the region of interest) as well as the behavior of such charge carrier under reaction conditions [32,33]. Fig. 4A presents two well-defined signals; one with apparently axial shape displaying $g_{\perp} \approx 1.99$ and unresolved parallel component, ascribable to Ti(III) species, and another orthorhombic with $g_1 = 2.016\text{-}7$, $g_2 = 2.011\text{-}2$; $g_3 \approx 2.002\text{-}4$, ascribable to trapped hole oxygen centers (O^- species), both of them typically formed in more or less hydrated anatase samples [32–36]. Both types of signals are also apparent already upon irradiation of the outgassed samples in the absence of oxygen (not shown) and do not change significantly upon subsequent oxygen introduction, suggesting that they basically correspond, in accordance with previous investigation [34], to subsurface species not easily involved in charge exchange with the media and thus, in chemical/biological-related steps. They are, however, long-lived electron/hole-derived radicals which certainly help to limit charge recombination in the oxide solid. Additionally, poorly resolved features at $g \approx 2.028$ and 2.024 reveal the formation of additional oxygen-derived species most likely originating from surface O^- and O_2^- species, respectively, in accordance with proposals in other works [33,34,36]. This adsorption, and therefore, the surface character of the corresponding radicals is confirmed by the absence of such EPR signals in the absence of oxygen gas. The overall amount of these surface radicals apparently decreases in the presence of silver in parallel to the metal content of the material. For the same silver content, photodeposited samples seem to display a lower quantity of oxygen radicals. Unfortunately, due to the relatively low intensity and poor resolution of these features, it is not possible to conclude on the effect of the silver content on their respective contribution to the spectra. In any case, the overall intensity decrease with increasing the silver content observed for this type of radicals in the samples of the two series, taking into account the essentially electron acceptor character of oxygen molecules [37], appears mainly a consequence of the electron trapping properties of silver [5,11], which thus appear only weakly dependent of the initial silver state. Sample 1.0AgF displays

evolution under light; Fig. 4B compares the fresh and used samples and a small increase in the overall intensity of electron/hole-derived trapped species generated under these conditions is apparent for the latter suggesting for it a certain hindering of the mentioned charge trapping properties of silver, although some greater contribution of electrical microwave absorption in the former cannot be discarded.

More conclusive results with respect to silver influence on differential electron/hole surface trapping capability are apparently achieved through DMPO spin-trapping experiments. As discussed in the introduction, *E. coli* membrane damage has been analyzed in detail and there is strong evidence that it occurs through hole-related radical attack, particularly involving OH-derived radicals [15,16,20]. A measure of the holes trapped at the material surface and involved in the microorganism inactivation can be thus obtained through the quantification of OH radicals. UV irradiation of DMPO-containing sample suspensions gives rise to a signal with 1:2:2:1 intensity pattern for all samples (Fig. 5A). Its EPR parameters ($g = 2.0056$, $a_N = 14.9$ G, $a_H = 14.9$ G) are characteristic of DMPO-OH adducts [35,38–41]. The intensity of the DMPO-OH adduct signal as a function of the time under UV irradiation is plotted in Fig. 5B. The TiO_2 single oxide reference displays a continuous growing behavior while photodeposited samples have a quick raising start followed by a smooth increase up to the end of the experiment. The impregnated samples, on the contrary, showed a maximum at relatively short times. The accumulation of DMPO-OH radical adducts seems thus to grow continuously in the first two cases (titania and photodeposited samples) but such radicals have more limited stability in the case of impregnated samples. The latter is likely an effect of multiple additions, within consecutive reactions, of OH radicals to DMPO molecules to yield diamagnetic species [35,38,41]. Differences among samples as a function of the preparation method are thus evident and can be ascribed to surface local differences in hole handling properties. No easy rationalization of the silver loading dependence of the radicals detected can be worked out from Fig. 5B; impregnated samples seems to decrease the overall number of adducts as well as progressively decreasing the amount of multiple additions inversely to the silver content while photodeposited samples display lesser differences with respect to the parent TiO_2 reference system. Since this analysis can be certainly complicated by the presence of the mentioned multiple radical interaction process yielding finally diamagnetic species, it is relevant noting that initial rates of DMPO-OH formation, which could be less affected by such process, follow the rate trend $TiO_2 < 1.0AgF < 0.5Ag < 2.5AgF \approx 2.5Ag < 1.0Ag$ (Fig. 5B inset). It can be noted here the good correlation between such initial inactivation rates and K_f values for the series prepared by impregnation; certainly, the presence of metallic silver in the high loading 2.5 wt.% catalysts prepared by photodeposition could explain, as detailed below, the absence of such correlation for this sample series. A last interesting point concerns the study of used samples depicted in Fig. 5C. While the impregnated 1.0Ag sample has a strong decay of intensity ascribable to the influence of surface occlusion by cell debris, such a behavior is absent from the 1.0AgF samples which, on the contrary, shows a moderate increase of the DMPO-OH adduct intensity. This latter can also be appreciably affected by the presence (fresh sample)/absence (used sample) of metallic silver (Fig. 2B) and its influence on the EPR measurement, as mentioned above. Considering now the results of Fig. 5C inset, we can see that the initial DMPO-OH adduct formation rates are in the order: $TiO_2 < 1.0Ag < 1.0AgF$.

4. Discussion

The analysis of the *E. coli* inactivation tests gives clear evidence of a key role of silver in the microorganism photokilling. Table 2 summarizes the experimental evidence and allows classifying the samples by the preparation method and silver content. As a general rule, samples mainly differ in the K_f inactivation rate and this drives the maximum log-reduction achieved. On the other hand, the slow step of the curves displayed in Fig. 3 is connected with additional (cell oxidative-stress response; cell debris blocking) phenomena. Thus, centering the analysis of Table 2 in the K_f values we can see three different situations as a function of the silver content. While samples below 1 wt.% display values nearly those observed for the reference material at dark conditions, the maximum K_f values are obtained for a 1 wt.% samples in both sample series. Above this loading, the two series have a different behavior and the photodeposited 2.5 wt.% sample (Table 2 and Fig. 3) is significantly better than its corresponding counterpart.

Silver can play several roles in the reaction. These roles have been previously unveiled by several works [5,7–10,12] and here we will study their appearance and/or dominance as a function of the silver content. On first place, we must recall here that the silver–titania interaction present in our 1 wt.% samples is enough to limit significant lixiviation within the reaction time, leaving this out of the possible roles of the noble metal in the maximization of the inactivation activity. Our titania-anatase has (surface) basic character [42] and a relatively high PZC (also called isoelectric point, IE). An IE point near or above 7 (e.g., basic character) is required to have optimum *E. coli* inactivation [43]. Our (maximum) silver content is too low to allow detection of significant IE changes (below 15%) with respect to our titania support, however, it clearly influences the surface adhesion properties of the system. Table 2 and Fig. 3 indicate that silver is mainly acting on the initial rate constant and that this parameter suffers the combined influence of the adhesion-chemical phenomenon and those of photo-physical nature. Adhesion of the bacteria is an important step of the reaction [44]. The comparison with dark tests suggests that the adhesion phenomenon is dominating the initial reaction behavior of the 0.5Ag catalyst, and that this phenomenon only has a modest influence with respect to the remaining contributions to the initial rate enhancement. Although silver would help increasing adhesion of bacteria to the titania surface, it seems that this silver-induced effect can only contribute in a modest way. This is in agreement with previous results, which showed the modest effect of silver on adhesion, at least with respect to the potential of other solids [44,45].

The photo-physical phenomena appear thus to dominate the behavior of our systems. Irrespective of the preparation method, maximum inactivation activity is obtained for the 1 wt.% content and is certainly connected with the influence of the oxidized silver entities present under reaction conditions in both 1.0 wt.% samples (Fig. 2B). Charge handling through the oxide–oxide interface is thus critical. Silver can act as an electron shrink while in contact with titania [5,11] and the EPR results reported in Fig. 4 support this fact, although through an oxide–oxide interface. No detailed mechanism can be put forward for such charge transfer, however, the comparison of the decreasing surface titania ability to capture electrons evidenced in Fig. 4 as the Ag content of the catalyst grows, and the *E. coli* inactivation results (Fig. 3) allow to dismiss a direct link between these two physical observables. In the case of the 2.5Ag, the presence of a metallic silver core powers the importance of the electron capture by the noble metal component and will limit charge recombination and increase the available number of holes (in agreement with comparison between photodeposited samples during OH radical trapping experiments displayed in Fig. 5B) able to interact with the microorganism. Although the enhanced electron capture by silver seems to support the limited loss of the photodeposited sample performance above

the 1 wt.% maximum in photodeposited samples with respect to the impregnated samples, it is clear that such phenomenon by itself does not explain the maximization of the photokilling behavior which occurs in the presence of essentially oxidized silver species. Electron capture by silver would thus contribute to enhance the *E. coli* inactivation capability of titania but does not explain the maximum of activity.

The above-mentioned discussion highlights the fact that silver-related TiO_2-charge unbalance upon light absorption and the higher availability of surface holes with respect to titania would thus not be the key parameter controlling bacteria inactivation; a detailed view of Fig. 5B in fact would indicate that modification of the hole properties can in fact be the key effect of the noble metal. All Ag-containing samples (photodeposited and impregnated) have OH radicals which apparently interact with DMPO in a different way than those of titania, with a faster, initial formation of the DMPO-OH adduct (Fig. 5B and C). The present results do not allow to further analyze this important issue but clearly unveil the fact that local differences in the configuration of OH species near silver entities are at the heart of the enhanced *E. coli* inactivation rates detected in the presence of silver. A detailed analysis of the TiO_2-surface OH groups responsible for radical creation by additional techniques is not an easy task as, for example, IR would not selectively study hydroxyl groups involved in radical generation upon light absorption. In any case, Fig. 5C showed that impregnated samples seem to suffer the deactivation of OH under reaction conditions possibly by the accumulation of cell debris during reaction. On the contrary, the silver oxidation state evolution detected in photodeposited samples would appear to lead to an increase of the hydroxyl radical formation. So, both samples evolve under reaction conditions, limiting such evolution to the local oxide–oxide interface in the case of impregnated samples plus a silver oxidation state evolution for photodeposited ones. Such changes influence the initial formation of the DMPO-OH adducts (inset of Fig. 5C) which appears to have a close relationship with the photokilling performance of the Ag–TiO_2 systems. Further time-resolved studies in the second region would be needed to further progress in this point.

5. Conclusions

The silver promotion of the TiO_2-anatase disinfection capability was investigated as a function of the preparation method, impregnation and photodeposition, and the noble metal content of the material. Using *E. coli* as a model microorganism, the study shows that a silver content around 1 wt.% maximizes the photokilling activity, irrespective of the preparation method. However, above this loading, photodeposited samples display improved performance. An analysis of the noble metal possible roles on the *E. coli* inactivation process allowed to rationalize these photocatalytic results. It was shown that silver changes the adhesion properties of the bacteria to the catalyst surface and can work as an electron shrink but both effects seem of limited importance to explain the whole set of results, although the latter would appear to significantly increase its importance for photodeposited samples with a silver content above 1 wt.%. The key property governing photokilling activity appears the local-type modification of hydroxyl radicals formed upon light absorption in the neighborhood of silver entities.

Acknowledgements

A.K. Thanks the CSIC for a postdoctoral I3P grant. The authors thank the CYCIT (CTQ2007-60480/BQU) and CSIC (PIF200580F0101) projects for financial support of this job.

References

[1] C.E. Laurence, P.R. Taylor, B.J. Truck, A.A. Reilly, Nat. Cancer Inst. 72 (1984) 365.
[2] M.R. Hoffmann, S.T. Martin, W. Choi, D.W. Bahnemann, Chem. Rev. 95 (1995) 69.
[3] J.-M. Herrmann, Topics Catal. 34 (2004) 49.
[4] O. Carp, C.L. Huisan, A. Reller, Prog. Solid State Chem. 32 (2004) 33.
[5] S.-K. Lee, A. Mill, Platinum Met. Rev. 47 (2003) 61.
[6] T. Matsunga, R. Tamada, H. Wake, FEBS Microbiol. Lett. 29 (1985) 211.
[7] J.C. Clement, J.S. Jarret, Metal-Based Drugs 1 (1994) 457.
[8] R.O. Fernández, R.A. Pizarro, Photochem. Photobiol. 64 (1996) 334.
[9] S. Lian, D. Read, W. Pugh, J. Furr, A. Russel, Lett. Appl. Microbiol. 25 (1997) 279.
[10] S. Thomas, P. McCubbin, J. Wound Care 12 (2003) 101.
[11] P. Kamat, J. Phys. Chem. B 106 (2002) 7729.
[12] H. Tada, T. Ishida, A. Takeo, S. Ito, Langmuir 20 (2004) 7898.
[13] H. Tran, K. Chiang, J. Scott, R. Amal, Photochem. Photobiol. 4 (2005) 565.
[14] A. Di Paola, E. García-López, G. Marci, C. Martin, L. Palmisano, V. Rives, A.M. Venezia, Appl. Catal. B 48 (2004) 223.
[15] J. Kiwi, V. Nadtochenko, Langmuir 21 (2005) 4631.
[16] V. Nadtochenko, N. Denisov, O. Sarkisov, D. Gumy, C. Pulgarin, J. Kiwi, J. Photochem. Photobiol. A 181 (2006) 401.
[17] A.G. Ricon, C. Pulgarin, Appl. Catal. B 44 (2004) 99.
[18] A.K. Benabbou, Z. Derriche, C. Felix, C. Guillard, Appl. Catal. B 76 (2007) 257.
[19] J.A. Ibañez, M.I. Litter, R.A. Pizarro, J. Photochem. Photobiol. A 157 (2003) 81.
[20] M. Cho, H. Chung, W. Choi, J. Yoon, Water Res. 38 (2004) 1069.
[21] A. Fuerte, M.D. Hernández-Alonso, A.J. Maira, A. Martínez-Arias, M. Fernández-García, J.C. Conesa, J. Soria, Chem. Commun. (2001) 2178.
[22] A. Fuerte, M.D. Hernández-Alonso, A.J. Maira, A. Martínez-Arias, M. Fernández-García, J.C. Conesa, J. Soria, J. Catal. 212 (2002) 1.
[23] M. Ferrer, J. Soliveri, F.J. Plou, N. López-Cortés, D. Reyes-Duarte, M. Christensen, J.L. Copa-Patiño, A. Ballesteros, Enzyme Microbial Technol. 36 (2005) 391.
[24] J. Jagger, Photchem. Photobiol. 34 (1981) 761.
[25] D. Mitoraj, A. Janaczyk, M. Strus, G. Stochel, P.B. Heazko, W. Macky, Photochem. Photobiol. Sci. 6 (2007) 642.
[26] M. Fernández-García, C. Belver, J.C. Hanson, X. Wang, J.A. Rodriguez, J. Am. Chem. Soc. 129 (2007) 13604.
[27] D. Lahiri, V. Subramanian, B.C. Bunker, P.V. Kamat, J. Chem. Phys. 124 (2006), n. 204720.
[28] P. Fernández-Ibáñez, J. Blanco, S. Malato, Water Res. 37 (2003) 3180.
[29] A. Kubacka, C. Serrano, M. Ferrer, E. Lunsford, P. Bielecki, M.L. Cerrada, M. Fernández-Garcia, M. Fernández-García, Nano Lett. (2007) 2529.
[30] L.A. Brook, P. Evans, H.A. Foster, M.E. Peble, A. Steele, D.W. Shwll, H.M. Yates, Photochem. Photobiol. A 187 (2007) 53.
[31] A.G. Rincón, C. Pulgarin, Catal. Today 101 (2005) 33.
[32] G. Colón, C. Belver, M. Fernández-García, Photocatalysis, in: M. Fernández-García, J.A. Rodríguez (Eds.), Synthesis, Properties and Application of Oxide Nanoparticles, Wiley, USA, 2007, , Chapter 17.
[33] C.P. Kumar, N.O. Gopal, T.C. Wang, H.-S. Wong, S.L. Ke, J. Phys. Chem. B 110 (2006) 5223.
[34] J.M. Coronado, A.J. Maira, J.C. Conesa, K.L. Yeung, V. Augugliaro, J. Soria, Langmuir 17 (2001) 5368.
[35] A. Fuerte, M.D. Hernández-Alonso, A. Iglesias-Juez, A. Martínez-Arias, J.C. Conesa, J. Soria, M. Fernández-García, Phys. Chem. Chem. Phys. 5 (2003) 2913.
[36] Y. Nakaoka, Y. Nosaka, J. Photochem. Photobiol. A 110 (1997) 299.
[37] M. Che, A.J. Tench, Adv. Catal. 32 (1983) 1.
[38] M.D. Hernández-Alonso, A.B. Hungría, A. Martínez-Arias, M. Fernández-García, J.M. Coronado, J.C. Conesa, J. Soria, Appl. Catal. B 50 (2004) 167.
[39] M.A. Grela, M.E.J. Coronel, A.J. Colussi, J. Phys. Chem. 100 (1996) 16940.
[40] E.G. Janzen, N. Sankuratry, Y. Kotake, J. Magn. Reson. 111 (1996) 254.
[41] D. Dvoranová, V. Brezová, M. Mazur, M.A. Malati, Appl. Catal. B 37 (2002) 91.
[42] C. Adan, A. Martínez-Arias, M. Fernández-García, A. Bahamonde, Appl. Catal. B 76 (2007) 395.
[43] D. Gumy, C. Morris, P. Bowen, C. Pulgarin, S. Giraldo, R. Hazdun, J. Kiwi, Appl. Catal. B 63 (2006) 76.
[44] B. Li, B.E. Logan, Colloid Surf. B 36 (2004) 81.
[45] M.R. Elahifard, S. Rahimnejad, S. Haghighi, M.R. Gholami, J. Am. Chem. Soc. 129 (2007) 9552.